

## Enhanced Production of Neutron-Rich Rare Isotopes in Peripheral Collisions at Fermi Energies

G. A. Souliotis, M. Veselsky, G. Chubarian, L. Trache, A. Keksis, E. Martin, D.V. Shetty, and S. J. Yennello

*Cyclotron Institute, Texas A&M University, College Station, Texas 77843, USA*

(Received 14 February 2003; published 8 July 2003)

A large enhancement in the production of neutron-rich projectile residues is observed in the reactions of a 25 MeV/nucleon  $^{86}\text{Kr}$  beam with the neutron-rich  $^{124}\text{Sn}$  and  $^{64}\text{Ni}$  targets relative to the predictions of the EPAX parametrization of high-energy fragmentation, as well as relative to the reaction with the less neutron-rich  $^{112}\text{Sn}$  target. A hybrid model based on a deep-inelastic transfer (DIT) code followed by a statistical deexcitation code accounts for part of the observed large cross sections. The DIT simulation indicates that the production of neutron-rich nuclides in these reactions is associated with peripheral nucleon exchange in which the neutron skins of the neutron-rich  $^{124}\text{Sn}$  and  $^{64}\text{Ni}$  target nuclei may play an important role. From a practical viewpoint, such reactions offer a novel synthetic avenue to access extremely neutron-rich rare isotopes towards the neutron-drip line.

DOI: 10.1103/PhysRevLett.91.022701

PACS numbers: 25.70.Hi, 25.70.Lm

Exploration of the nuclear landscape towards the neutron-drip line [1] is currently of great interest in order to elucidate the evolution of nuclear structure with increasing neutron-to-proton ratio ( $N/Z$ ) [2,3] and understand important nucleosynthesis pathways [4], most notably the  $r$  process [5]. Reactions induced by neutron-rich nuclei provide invaluable information on the isospin dependence of the nuclear equation of state [6,7]. Extremely neutron-rich nuclei offer the unprecedented opportunity to extrapolate our knowledge to the properties of bulk isospin-rich matter, such as neutron stars [8,9]. The efficient production of very neutron-rich nuclides is a key issue in current and future rare isotope beam facilities around the world [10–12] and, in parallel, the search for new synthetic approaches is of exceptional importance.

Neutron-rich nuclides have traditionally been produced in spallation reactions, fission, and projectile fragmentation [13]. In high-energy fragmentation reactions, the production of the most neutron-rich isotopes is based on a “clean-cut” removal of protons from the projectile. The world’s data on fragmentation cross sections are well represented by the empirical parametrization EPAX (experimental parametrization of cross sections) [14]. EPAX is currently the common basis for predictions to plan rare beam experiments and facilities. In addition to the widely used projectile fragmentation approach, neutron-rich nuclides can be produced in multinucleon transfer reactions [15] and deep-inelastic reactions near the Coulomb barrier (e.g., [16–18]). In such reactions, the target  $N/Z$  significantly affects the production cross sections, but the low velocities of the fragments and the ensuing wide angular and ionic charge state distributions render practical applications rather limited.

The Fermi energy regime (20–40 MeV/nucleon) [19] offers the unique opportunity to combine the advantages of both low- and high-energy reactions. At this energy, the synergy of projectile and target enhances the  $N/Z$  of the fragments, while the velocities are high enough to

allow efficient in-flight collection and separation. Early work on neutron-rich fragment production from heavy projectiles at Fermi energies [20–22] provided no production cross sections, hampering quantitative comparisons to parametrizations, or reaction simulations. In order to explore the possibilities offered at Fermi energies, we recently undertook an experimental study of the production cross sections of projectile residues from the reaction 25 MeV/nucleon  $^{86}\text{Kr} + ^{64}\text{Ni}$ , in which enhanced production of neutron-rich fragments was observed [23].

In this Letter, we focus on a subsequent detailed study of near-projectile residues from the reactions of  $^{86}\text{Kr}$  (25 MeV/nucleon) with  $^{124}\text{Sn}$  and  $^{112}\text{Sn}$  targets and present a comparison with the results from  $^{86}\text{Kr} + ^{64}\text{Ni}$  [23], as well as with the expectations of EPAX [14]. We demonstrate that the production of neutron-rich projectile residues is substantially enhanced in the reactions involving the most neutron-rich systems and we provide an interpretation based on a deep-inelastic transfer model.

The measurements were performed at the Cyclotron Institute of Texas A&M University, following the experimental scheme of our previous work [23]. A concise description is given in the following. A 25 MeV/nucleon  $^{86}\text{Kr}^{22+}$  beam ( $\sim 1$  pA) from the K500 superconducting cyclotron interacted with  $^{124}\text{Sn}$  and  $^{112}\text{Sn}$  targets (2 mg/cm<sup>2</sup>). Projectile residues were analyzed with the Momentum Achromat Recoil Separator (MARS) [24] offering an angular acceptance of 9 msr and momentum acceptance of 4%. The beam struck the target at 4.0° relative to the optical axis of MARS. Thus, fragments were accepted in the polar angular range 2.7°–5.4° (lying inside the grazing angle of 6.5° for the Kr + Sn reaction at 25 MeV/nucleon). At the MARS focal plane, the fragments were collected in a two-element ( $\Delta E, E$ ) Si detector telescope. Time of flight was measured between two PPACs (parallel plate avalanche counters) placed at the MARS dispersive image and at the focal plane,

respectively. The horizontal position from the first PPAC and the field of the MARS first dipole magnet determined the magnetic rigidity,  $B\rho$ . The fragments were characterized event by event by energy loss, residual energy, time of flight, and  $B\rho$ . With the procedures described in Ref. [23], the atomic number  $Z$ , the ionic charge  $q$ , the mass number  $A$ , and the velocity were obtained with high resolution (0.5, 0.4, 0.6 units and 0.3%, respectively). After summation over ionic charge states (with corrections for missing charge states), fragment cross sections with respect to  $Z$ ,  $A$ , and velocity were obtained in the angular range  $2.7^\circ$ – $5.4^\circ$  and  $B\rho$  range 1.3–2.0 Tm. To extract total cross sections, the measured yield data were corrected for the limited angular acceptance and magnetic rigidity range covered. The corrections were obtained from the ratio of the total to the filtered cross sections (with angular and momentum acceptance cuts) calculated using the simulation approach described below. The corrections involved an azimuthal angular factor of 10 and mass-dependent polar factors ranging from 2 to 4 for  $A = 85$  to 50, respectively (resulting in, e.g., a total factor of 20 for fragments very close to the projectile). The systematic uncertainty in the extracted cross sections is estimated to be a factor of 2 [23].

Figure 1 shows the results of the mass distributions (cross sections) of elements  $Z = 30$ – $35$  from the reactions of  $^{86}\text{Kr}$  (25 MeV/nucleon) with  $^{124}\text{Sn}$  (full circles) and  $^{112}\text{Sn}$  (full squares). The dotted lines are the predictions of the EPAX parametrization [14]. We observe that the neutron-rich projectile fragments produced in the reaction with the more neutron-rich  $^{124}\text{Sn}$  ( $N/Z = 1.48$ ) target have considerably larger yields compared to those obtained in the reaction with the less neutron-rich  $^{112}\text{Sn}$  target ( $N/Z = 1.24$ ). Typical ratios are 3–10 for the most neutron-rich isotopes observed in both reactions. In most of the cases of the present data, the most neutron-rich nuclides have been observed only in the  $^{86}\text{Kr} + ^{124}\text{Sn}$  reaction. Compared to EPAX, the yields from  $^{86}\text{Kr} + ^{124}\text{Sn}$  are substantially larger, whereas those from  $^{86}\text{Kr} + ^{112}\text{Sn}$  are in reasonable agreement with EPAX. It should be pointed out that EPAX represents an abrasion-ablation type of fragmentation scenario in which the target is a mere spectator having (almost) no effect on the production cross section (apart from a geometrical factor) [14]. To quantify the comparison between the present data and EPAX, we show in Fig. 2(a) the ratio of the measured cross sections of fragments with  $Z = 28$ – $35$  from  $^{86}\text{Kr} + ^{124}\text{Sn}$  with respect to EPAX expectations. The same ratio is presented in Fig. 2(b) for our previous data on  $^{86}\text{Kr} + ^{64}\text{Ni}$  [23]. In the EPAX calculation, we extended the prediction up to one neutron pickup product to allow comparison with the present data. However, our data on  $^{86}\text{Kr} + ^{124}\text{Sn}$  and  $^{86}\text{Kr} + ^{64}\text{Ni}$  show the production of nuclides with up to 3–4 neutrons picked up from the target, along with the usual proton removal products. In both figures, we observe that for nuclei far from the projectile ( $Z = 28$ – $30$ ), as well as for  $N/Z$  less than that

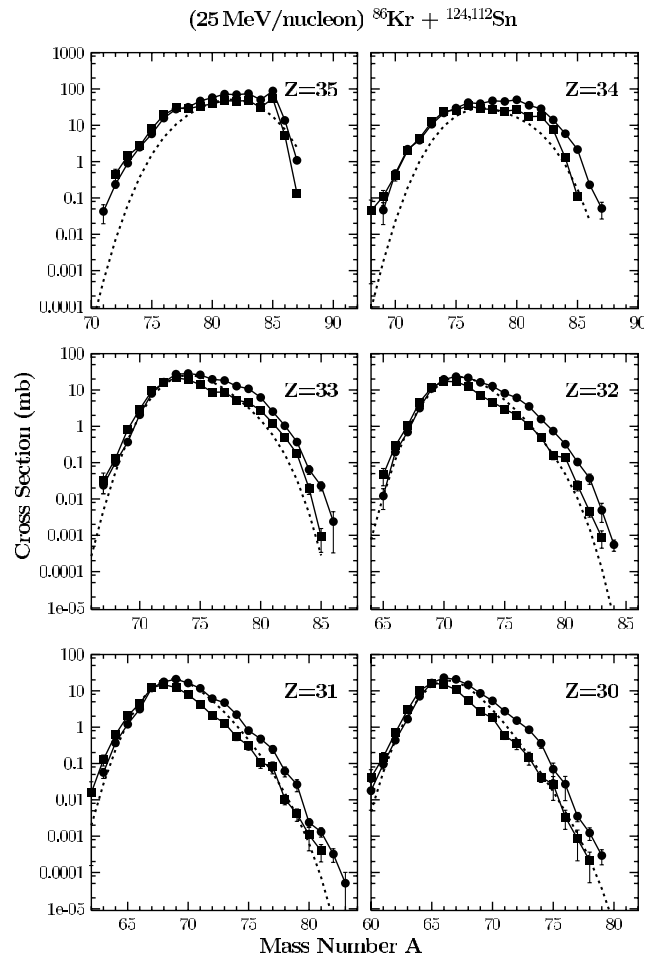


FIG. 1. Mass distributions of elements  $Z = 30$ – $35$  from the reaction of  $^{86}\text{Kr}$  (25 MeV/nucleon) with  $^{124}\text{Sn}$  and  $^{112}\text{Sn}$ . The data are shown by full circles for  $^{86}\text{Kr} + ^{124}\text{Sn}$  and full squares for  $^{86}\text{Kr} + ^{112}\text{Sn}$ . The dotted lines are EPAX expectations [14].

of the projectile ( $N/Z = 1.39$ , arrow in Fig. 2), the experimental cross sections are in remarkable agreement with EPAX (within a factor of  $\sim 2$ ). However, for heavier elements ( $Z = 31$ – $35$ ) and for progressively higher  $N/Z$ , a striking increase in the ratio is observed, especially for near-projectile products involving neutron pickup. The observed yield amplification over EPAX for neutron-rich nuclei demonstrates the dramatic effect of the neutron-rich target on the production mechanism at Fermi energies, which involves substantial nucleon exchange [25].

To gain insight into the mechanism of neutron-rich nuclide production at this energy, we performed simulations using a hybrid Monte Carlo approach, as in [23]. The dynamical stage of the collision was described by the deep-inelastic transfer (DIT) code of Tassan-Got [26] and the deexcitation stage was simulated by the statistical code GEMINI [27]. Comparison of the DIT/GEMINI predictions with the data is shown in Fig. 3 for Se ( $Z = 34$ ), Ge ( $Z = 32$ ), and Zn ( $Z = 30$ ) (thick solid lines). We observe that the calculation describes well, in most cases, the

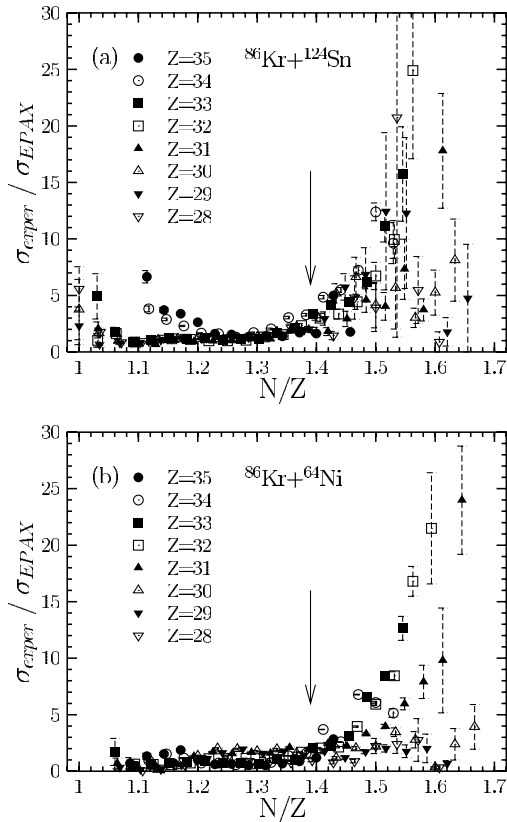


FIG. 2. Ratio of measured cross sections of projectile residues from  $^{86}\text{Kr}$  (25 MeV/nucleon) on  $^{124}\text{Sn}$  target (a) (current measurement), and on  $^{64}\text{Ni}$  target (b) [23] with respect to EPAX expectations [14]. Arrows indicate the  $N/Z$  of the projectile.

central and the neutron-deficient part of the measured distributions. However, it cannot fully account for the enhancement observed on the neutron-rich sides for near-projectile elements. Backtracing of the DIT simulations indicates that neutron-rich products originate in peripheral collisions in which the projectile-target density distributions overlap by up to 1–1.5 fm. For larger projectile-target overlaps, the observed enhancement diminishes and the cross sections agree with DIT/GEMINI [23] and EPAX (Fig. 2). It is worth noting the large cross sections from  $^{86}\text{Kr} + ^{64}\text{Ni}$  [23] relative to  $^{86}\text{Kr} + ^{112}\text{Sn}$ , although the targets have nearly equal  $N/Z$ . In this case it is their position with respect to the valley of  $\beta$  stability ( $^{64}\text{Ni}$  is neutron rich and  $^{112}\text{Sn}$  is neutron poor) that determines the nucleon flow. Consequently, the potential energy surface (appropriately taken into account in the DIT code) plays a definitive role in the production of neutron-rich fragments at Fermi energies.

We should point out that, in the original DIT code [26], the nuclei are assumed spherical with homogeneous neutron and proton density distributions. However, it is well established that neutron-rich nuclei possess neutron skins; namely, their neutron density distributions extend further out relative to the proton distributions. As is well known, the neutron skin is predicted by a variety of

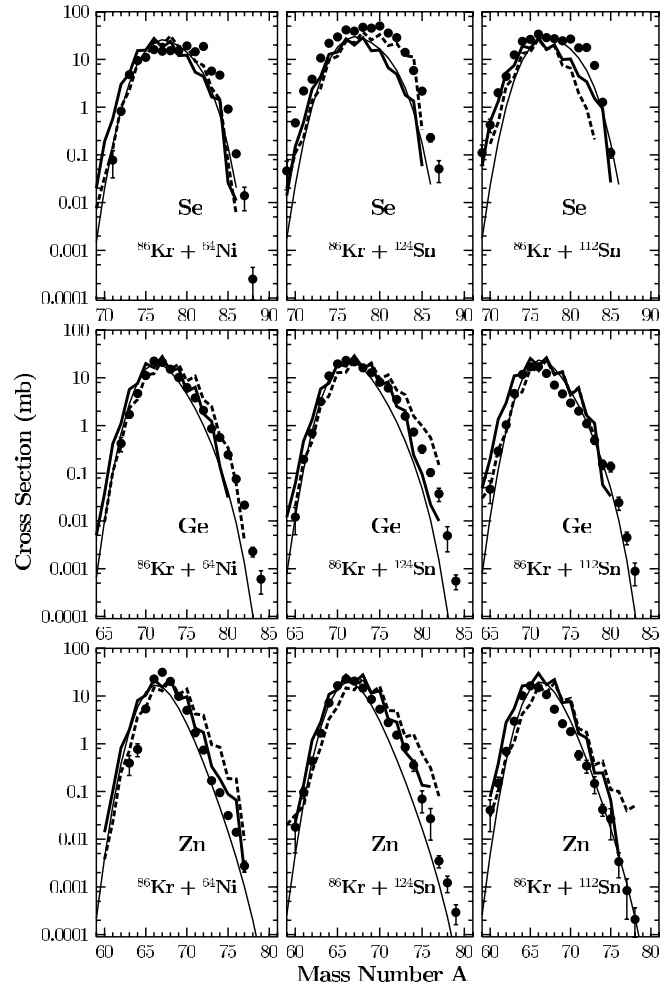


FIG. 3. Comparison of experimental mass distributions of Se ( $Z = 34$ ), Ge ( $Z = 32$ ), and Zn ( $Z = 30$ ) from  $^{86}\text{Kr}$  (25 MeV/nucleon) on  $^{64}\text{Ni}$  [23],  $^{124}\text{Sn}$ , and  $^{112}\text{Sn}$  (present data) with DIT/GEMINI calculations without (thick solid line) and with (thick dashed line) neutron and proton density distributions. The thin solid line is the EPAX prediction [14].

theoretical models including microscopic Thomas-Fermi, Skyrme Hartree-Fock, and relativistic mean-field approaches (e.g., [28–30]). Also, it has recently been demonstrated experimentally in annihilation studies of antiprotonic atoms [31]. Some time ago, Harvey [32] took into consideration the neutron skin of heavy targets ( $^{208}\text{Pb}$ ,  $^{197}\text{Au}$ ) in a microscopic nucleon-nucleon scattering model to explain the enhanced production of neutron-rich projectile fragments from  $^{16}\text{O}$  and  $^{20}\text{Ne}$  at Fermi energies relative to those at relativistic energies. His approach also served as an interpretation of the  $N/Z$  properties of projectile fragment yield data from  $^{40}\text{Ar}$  (44 MeV/nucleon) on heavy targets [22]. Although the DIT code employed in our simulations is based on nucleon exchange (rather than nucleon-nucleon collisions) in the overlap zone, we may attribute its partial success to describe the observed enhanced cross sections to the inadequate treatment of peripheral nucleon exchange, in which the neutron skins of the reaction partners may play

important roles. To investigate this assumption further, we included neutron and proton density distributions into the DIT code. The density distributions were calculated with a microscopic Thomas-Fermi code [28] and employed in DIT. In the simulation, at a given projectile-target overlap and a given nucleon exchange site, the transfer probabilities were scaled by the local peripheral (“halo”) factors,  $(\rho_n/\rho_p)/(N/Z)$ , of the respective reaction partners. The change of the density profiles was followed during the (sequential) nucleon exchange. The results of this modified-DIT/GEMINI calculation are shown in Fig. 3 by dashed lines. A qualitative improvement in the description of the neutron-rich sides of the distributions for near-projectile elements from the very neutron-rich systems  $^{86}\text{Kr} + ^{64}\text{Ni}$  and  $^{86}\text{Kr} + ^{124}\text{Sn}$  is found. However, for the  $^{86}\text{Kr} + ^{112}\text{Sn}$  reaction, the standard DIT/GEMINI calculation agrees better with the data. These calculations indicate, although qualitatively, the possible effect of the neutron skin of the neutron-rich targets  $^{64}\text{Ni}$  and  $^{124}\text{Sn}$  in the observed enhancement. Guided by these observations, we infer that an improved deep-inelastic transfer model, or an equivalent approach, which self-consistently takes into account the neutron and proton density distributions of the reaction partners may account for the large cross sections of the neutron-rich products observed in such reactions.

From a practical viewpoint, the large production cross section of neutron-rich fragments indicate that such reactions offer an attractive approach to produce very neutron-rich nuclides. Apart from direct in-flight or ion-guide isotope separation on-line (IGISOL)-type options, we propose the application of such reactions as a second stage in two-stage rare beam production schemes. For example, a beam of  $^{92}\text{Kr}$  from an ISOL-type facility [or, from the proposed rare isotope accelerator facility [10,11]] can be accelerated around the Fermi energy and interact with a very neutron-rich target (e.g.,  $^{64}\text{Ni}$ ,  $^{124}\text{Sn}$ ,  $^{208}\text{Pb}$ ,  $^{238}\text{U}$ ) to produce extremely neutron-rich nuclides that cannot be accessed by fission or projectile fragmentation. A quantitative prediction of rates of such nuclides will be possible after further experimental studies and improvement of the description of peripheral collisions between very neutron-rich heavy nuclei in the Fermi energy regime.

In summary, a substantial enhancement in the production cross sections of neutron-rich projectile fragments is observed in the reactions  $^{86}\text{Kr}$  (25 MeV/nucleon) +  $^{124}\text{Sn}$  and  $^{86}\text{Kr}$  (25 MeV/nucleon) +  $^{64}\text{Ni}$  relative to the EPAX parametrization, as well as relative to the less neutron-rich system  $^{86}\text{Kr} + ^{112}\text{Sn}$ . The hybrid DIT/GEMINI model provides a partial interpretation of the observed cross sections. The DIT simulations indicate that the enhanced production of neutron-rich isotopes in the reactions  $^{86}\text{Kr} + ^{124}\text{Sn}$  and  $^{86}\text{Kr} + ^{64}\text{Ni}$  is associated with peripheral nucleon exchange. In such collisions, the neutron skins of the  $^{124}\text{Sn}$  and  $^{64}\text{Ni}$  target nuclei may play a significant role. For practical purposes, such reactions

offer a novel and competitive pathway to produce extremely neutron-rich isotopes towards the neutron-drip line.

We are thankful to L. Tassan-Got for his DIT code and useful suggestions. We also thank A. Sanzhur for insightful discussions and R. Charity for the use of the GEMINI code. We gratefully acknowledge the support of the operations staff of the Cyclotron Institute during the measurements. Financial support for this work was provided, in part, by the U.S. Department of Energy under Grant No. DE-FG03-93ER40773 and by the Robert A. Welch Foundation under Grant No. A-1266.

- 
- [1] P. Moller, J. R. Nix, and K. L. Kratz, *At. Data Nucl. Data Tables* **66**, 131 (1997).
  - [2] R. F. Casten and B. M. Sherrill, *Prog. Part. Nucl. Phys.* **45**, 171 (2000).
  - [3] J. Meng and P. Ring, *Phys. Rev. Lett.* **80**, 460 (1998).
  - [4] C. Sneden and J. J. Cowan, *Science* **299**, 70 (2003).
  - [5] K. Langanke and M. Wiescher, *Rep. Prog. Phys.* **64**, 1657 (2001).
  - [6] P. Danielewicz, R. Lacey, and W. G. Lynch, *Science* **298**, 1592 (2002).
  - [7] B.-A. Li, *Phys. Rev. C* **66**, 034609 (2002).
  - [8] C. J. Pethick and D. G. Ravenhall, *Annu. Rev. Nucl. Part. Sci.* **45**, 429 (1995).
  - [9] T. Sil *et al.*, *Phys. Rev. C* **66**, 045803 (2002).
  - [10] D. J. Morrissey, *Eur. Phys. J. A* **15**, 105 (2002).
  - [11] J. A. Nolen, *Eur. Phys. J. A* **13**, 255 (2002).
  - [12] D. Guereau, *Eur. Phys. J. A* **13**, 263 (2002).
  - [13] H. Geissel and G. Munzenberg, *Annu. Rev. Nucl. Part. Sci.* **45**, 163 (1995).
  - [14] K. Sümmerer and B. Blank, *Phys. Rev. C* **61**, 034607 (2000).
  - [15] L. Corradi *et al.*, *Nucl. Phys.* **A701**, 109 (2002).
  - [16] R. Broda, *Eur. Phys. J. A* **13**, 1 (2002).
  - [17] V. V. Volkov, *Phys. Rep.* **44**, 93 (1978).
  - [18] I. Y. Lee *et al.*, *Phys. Rev. C* **56**, 753 (1997).
  - [19] H. Fuchs and K. Möhring, *Rep. Prog. Phys.* **57**, 231 (1994).
  - [20] C. O. Bacri *et al.*, *Nucl. Phys.* **A555**, 477 (1993).
  - [21] D. Bazin *et al.*, *Nucl. Phys.* **A515**, 349 (1990).
  - [22] V. Borrel *et al.*, *Z. Phys. A* **324**, 205 (1986).
  - [23] G. A. Souliotis *et al.*, *Phys. Lett. B* **543**, 163 (2002).
  - [24] R. E. Tribble, R. H. Burch, and C. A. Gagliardi, *Nucl. Instrum. Methods Phys. Res., Sect. A* **285**, 441 (1989).
  - [25] M. Veselsky *et al.*, *Phys. Rev. C* **62**, 064613 (2000).
  - [26] L. Tassan-Got and C. Stefan, *Nucl. Phys.* **A524**, 121 (1991).
  - [27] R. Charity *et al.*, *Nucl. Phys.* **A483**, 371 (1988).
  - [28] V. M. Kolomietz, A. I. Sanzhur, S. Shlomo, and S. A. Firin, *Phys. Rev. C* **64**, 024315 (2001).
  - [29] B. A. Brown, *Phys. Rev. C* **58**, 220 (1998).
  - [30] F. Hofmann, C. M. Keil, and H. Lenske, *Phys. Rev. C* **64**, 034314 (2001).
  - [31] A. Trzcinska *et al.*, *Phys. Rev. Lett.* **87**, 082501 (2001).
  - [32] B. G. Harvey, *Nucl. Phys.* **A444**, 498 (1985).